



Electrical conductivity study in pure and doped ZnO ceramic system

Ayman Sawalha, M. Abu-Abdeen¹, A. Sedky^{*,2}

Physics Department, Faculty of Science, King Faisal University, Al-Hassa 31982, P.O. Box 400, Saudi Arabia

ARTICLE INFO

Article history:

Received 2 November 2008
Received in revised form
6 December 2008
Accepted 12 December 2008

Keywords:

Conductivity
Jumps
Activation energy
Low and high and Fe doped ZnO

ABSTRACT

We report here the electrical conductivities measurements of $Zn_{1-x}Fe_xO$ ceramic samples with various x values ($0.00 \leq x \leq 0.50$). The measurements are made in both high and low temperature cases ($300 K \leq T \leq 523 K$) and ($20 K \leq T \leq 300 K$), respectively. Furthermore, the electrical conductivity data are well enough to calculate the activation energies E_a for the considered samples. The character of the conductivities curves is not absolutely symmetric to the response of temperature in both cases. Interestingly, two jumps are observed only in the conductivity curves at low temperatures. The onset temperatures of these jumps are increased by Fe up to 0.30, followed by a decrease at Fe = 0.50. At constant Fe content, the conductivities are found to be increased over the temperature range in both cases. While, these values are decreased with the increase in the Fe content up to Fe = 0.50. The conductivity character is divided into discrete regions over the temperature range corresponding to different activation energies. In high temperature case, the values of E_a are increased with increasing Fe up to 0.30, followed by a decrease at 0.50. While, in low temperature cases, the values of E_a are generally increased with increasing Fe up to 0.50. Our results are discussed in terms of potential barrier, donor concentration, point defects and adsorption–desorption of oxygen which are affected by Fe doping in ZnO ceramic system.

© 2009 Elsevier B.V. All rights reserved.

1. Introduction

Zinc oxide (ZnO) based varistor exhibits strong n-type conductivity with the electrons to move in the conduction band as charge carriers. Typical ZnO based varistor is a very complex chemical system containing several different dopants [1–6]. The electrical properties of ZnO are dependent on the composition and on microstructural characteristics, such as grain size, density, morphology and the distribution of second phases. The effect of dopants on the electrical properties of ZnO varistor has been investigated by several researchers [7–13]. It has been observed that the region of nonlinearity of Al doped ZnO can be extended to higher applied fields and consequently the conductivity of ZnO grains is improved [12]. While the conductivity of ZnO has decreased by the doping of both Co, Mn and Cu dopants, and the samples still showed a semiconductor behavior [12,13].

Although, there are few reports on the doping elements in the ZnO varistor, the effects of some dopants such as Fe on the electrical conductivity of ZnO varistor still remain unclear. This is because the doping effects have been studied in quite different

systems under different experimental conditions. Therefore, it is necessary to investigate the Fe independently in a systematic way to understand the role of Fe doping in the electrical conductivity of ZnO varistor. Recently, Sedky et al. [14] have presented in detail the effects of Fe doping on structural and I – V characteristics of ZnO samples. It is found that the addition of Fe improved the nonlinear properties of ZnO varistor and the electrical barriers could be formed. In this work, the temperature effect electrical conductivity is investigated on the same batch of samples. The measurements of electrical conductivity are performed in both high and low temperature cases, respectively. From electrical conductivity measurements the activation energies are calculated and discussed for all samples.

2. Experimental details

Samples of the series $Zn_{1-x}Fe_xO$ with various x values are synthesized by using conventional solid state reaction method. The powders of ZnO and Fe_2O_3 (Aldrich 99.999 purity) are thoroughly mixed in required proportions and calcined at $900^\circ C$ in air for a period of 12 h. The resulting powders are ground, mixed, and pressed into disks of 1 cm diameter and 0.5 cm thick. Two disks are made for each composition. The pellets are then sintered at $1000^\circ C$ for a period of 8 h. Finally, one set of samples are quenched from sintering temperature down to room temperature, while the other is left in the furnace and slowly

* Corresponding author.

E-mail address: sedky1960@yahoo.com (A. Sedky).

¹ Permanent address: Physics Department, Faculty of Science, Cairo University, Giza, Egypt.

² Permanent address: Physics Department, Faculty of Science, Assiut University, Assiut, Egypt.

cooled to room temperature. The dc electrical resistivity measurements at high temperature (300–523 K) are measured with an electrometer (model 6517, Keithley) and 5 kV dc power supply. High quality silver paint is used on the samples surfaces for electrical contacts. While the dc electrical resistivity measurements at low temperatures ($20\text{ K} \leq T \leq 300\text{ K}$) are measured in closed cycle refrigerator (Cryomech compressor package with cryostat Model 810-1812212, USA) within the range of 20–300 K. Nanovoltmeter Keithley 2182, current source Keithley 6220 and

temperature controller 9700 (0.001 K resolution) are used in this experiment.

3. Discussion

3.1. Background

It is well known that electrical conductivity of ZnO samples is controlled by the intrinsic defects generated at high temperature and also by the presence of dopants, either specifically added to the materials or not. During the cooling of the samples, the defects tend to migrate to the grain boundaries and annihilated (intrinsic

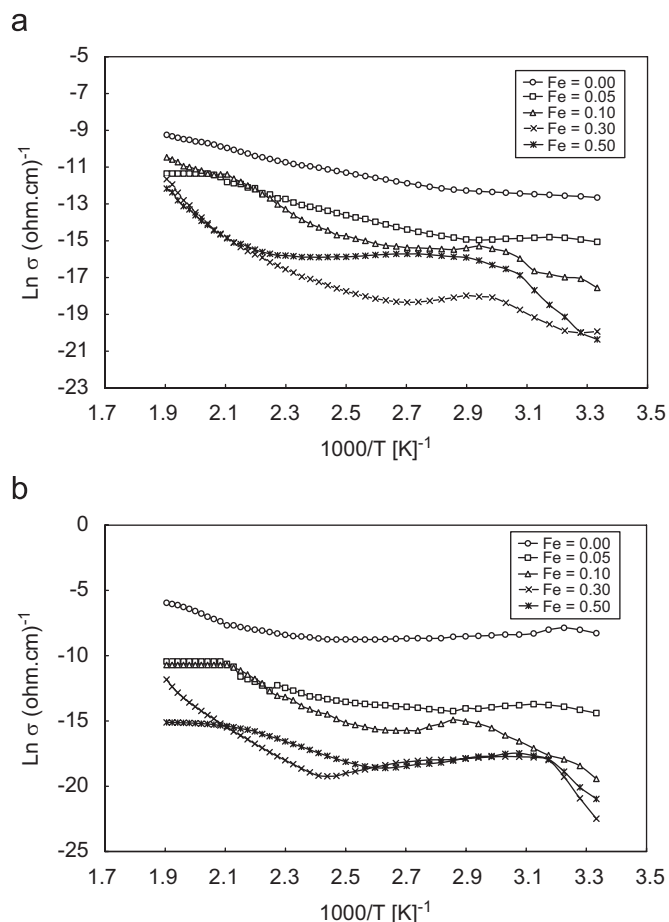


Fig. 1. (a) Electrical conductivity versus $1000/T$ for quenched $\text{Zn}_{1-x}\text{Fe}_x\text{O}$ samples at high temperatures: HT quenching and (b) electrical conductivity versus $1000/T$ for slowly cooled $\text{Zn}_{1-x}\text{Fe}_x\text{O}$ samples at high temperatures: HT slow cooling.

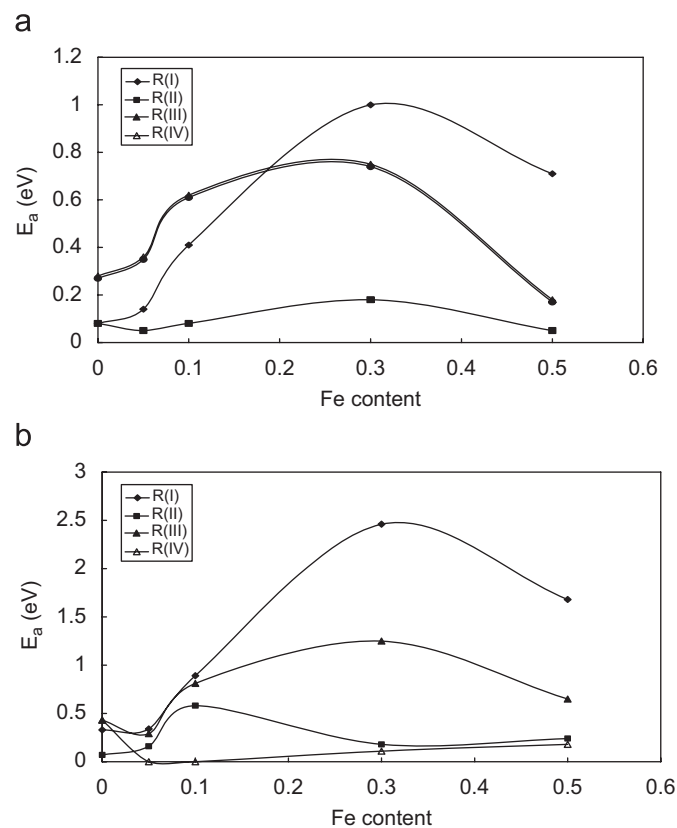


Fig. 2. (a) Activation energy versus Fe content for $\text{Zn}_{1-x}\text{Fe}_x\text{O}$ quenched samples at high temperatures: HT quenching and (b) activation energy versus Fe content for $\text{Zn}_{1-x}\text{Fe}_x\text{O}$ slowly cooled samples at high temperatures: HT slow cooling.

Table 1

E_a versus Fe content at high temperature for $\text{Zn}_{1-x}\text{Fe}_x$ samples in both quenching and slow cooling.

Fe content	E_a (I) eV (300–325 K)	E_a (II) eV (330–390 K)	E_a (III) eV (395–460 K)	E_a (IV) eV (460–525 K)
Quenching				
0.00	0.08	0.08	0.27	0.28
0.05	0.14	0.05	0.35	0.36
0.10	0.41	0.08	0.61	0.62
0.30	1.00	0.18	0.74	0.75
0.50	0.73	0.05	0.17	0.18
Slow cooling				
0.00	0.33	−0.07	0.43	0.43
0.05	0.34	−0.16	0.29	0.00
0.10	0.89	−0.58	0.81	0.00
0.30	2.46	−0.18	1.25	0.12
0.50	1.68	0.24	0.65	0.18

defects) or to be exsolved if their solubility limit is attained (extrinsic effects). This migration process is normally slow and is thermally activated, meaning that at some temperatures, not much lower than the sintering one, only the defects near the grain boundaries are effectively eliminated. The resulting concentration profiles considerably affect the electrical properties of ZnO varistor [12,15]. In order to avoid this process, samples are quenched from sintering temperature down to room temperature. On doing this, we can assume that at room temperature the defects are homogeneously distributed in the material, and their concentration are the same as those at the sintering temperature, except for electrons and holes which can readily diffuse at room temperature. For a comparison, another set of samples are left in the furnace for slow cooling. After doing this step, the resistivity versus temperature measurements is performed in both high and low temperature case. The values of resistivity are used for calculating the electrical conductivity of the considered samples in both quenching and slow cooling.

3.2. High temperature measurements

Fig. 1(a and b) shows the variation of dc electrical conductivity $\ln \sigma$ of pure and Fe doped ZnO samples with temperature as $1000/T$ ($300\text{ K} \leq T \leq 525\text{ K}$) in both quenching and slow cooling. It is clear that the conductivity decreased with the increase in the Fe content in both cases, while the conductivity is increased

significantly with temperature and became considerably higher than its values at room temperature. There is a curvature in the conductivity curves observed at 325 K for all Fe doped samples. However, it was observed that the densities of Fe doped ZnO samples decreased with increasing Fe content [14]. This means that Fe doping produce a large amount of pores which may be the main reason for the significant decrease in the conductivity of the considered samples. On the other hand, the solid solution of Fe in ZnO samples may become the main influencing factor on the increasing of conductivity with temperature at constant Fe content [15]. It is well known that the trivalent ion can be dissolved in ZnO, acts as a shallow donor and should increase the conductivity of ZnO [7,16]. Anyhow, the results of conductivities showed that when Fe is dissolved in ZnO, it behaves as a deep donor and depresses the concentrations of the intrinsic donors at sintering temperatures. When the samples either quenched or slowly cooled, the concentrations of intrinsic donors at room temperature are also lowered [15,20–23]. In this way, the room temperature electrical conductivity is lowered by the presence of Fe doping. With increasing temperature the Fe deep donors may start to ionize, resulting in an increase in the room temperature conductivity. Furthermore, with increasing temperature, the concentrations of native defects, namely the intrinsic donors' defects, increase which results in the increase of the conductivity.

Anyhow, many researchers have studied the effects of 3d transition metal impurities on the electrical conductivity of ZnO varistor. They investigate that these metals could enhance the

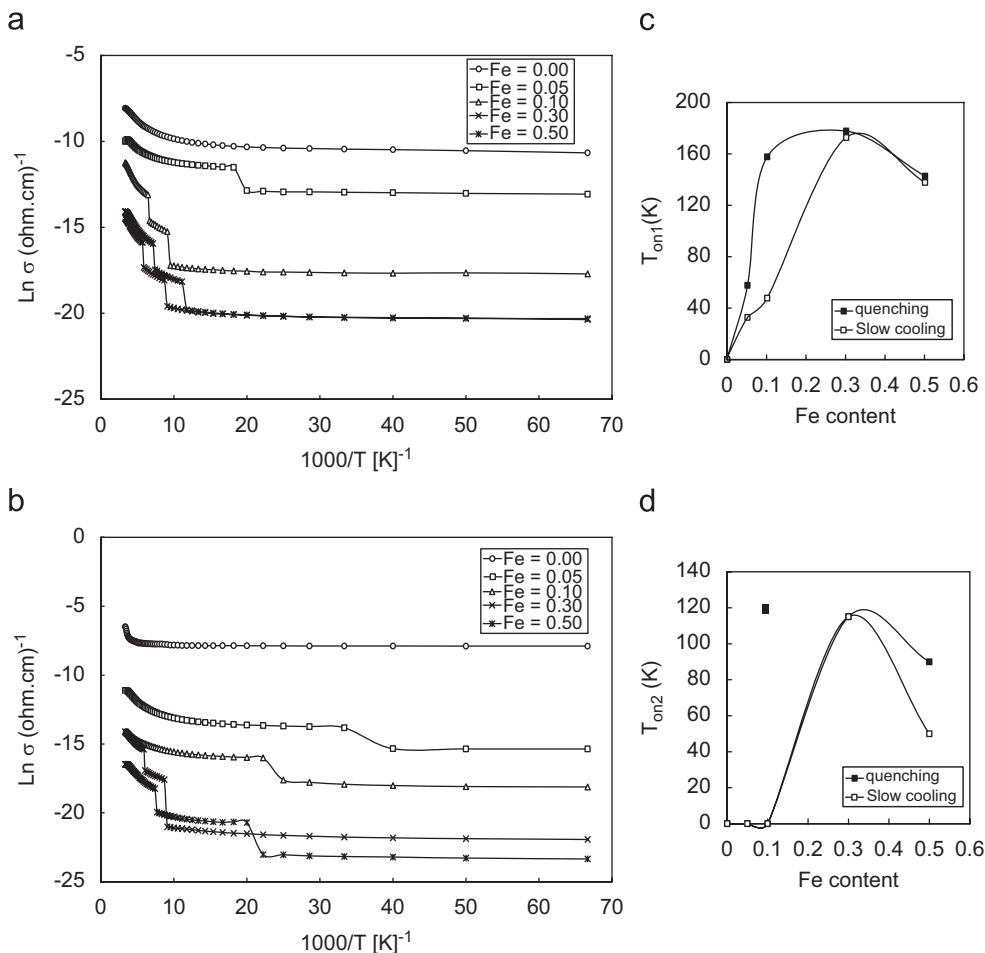


Fig. 3. (a) Electrical conductivity versus $1000/T$ for $\text{Zn}_{1-x}\text{Fe}_x\text{O}$ quenched samples at low temperatures: LT quenching; (b) electrical conductivity versus $1000/T$ for slowly cooled $\text{Zn}_{1-x}\text{Fe}_x\text{O}$ samples at low temperatures LT slow cooling; (c) the onset temperature of first jump versus Fe content for $\text{Zn}_{1-x}\text{Fe}_x\text{O}$ samples at low temperatures and (d) the onset temperature of second jump versus Fe content for $\text{Zn}_{1-x}\text{Fe}_x\text{O}$ samples at low temperatures.

excess oxygen concentration in the grain boundary region and a potential barrier is formed preferentially [17–19]. Therefore, the electrical conductivity of the Fe doped ZnO samples is apparently lower than that of the undoped ZnO, and the grain boundary is more resistive than the grain. Then Fe can be used in the ZnO varistor to build up the potential barrier in the grain boundary, in agreement with our previous investigation [14].

The conductivity–temperature dependence is subjected to the conventional relation;

$$\sigma = \sigma_0 e^{-E_a/kT} \quad (1)$$

where σ and σ_0 are the electrical conductivities at temperatures T and 0K , respectively. Within the temperature range selected for the conductivity measurements, it is possible to distinguish discrete regions corresponding to different activation energies. The character is divided into four regions over the temperature intervals as follows; ($300\text{K} \leq T \leq 330\text{K}$), ($330\text{K} \leq T \leq 390\text{K}$), ($390\text{K} \leq T \leq 450\text{K}$) and ($450\text{K} \leq T \leq 525\text{K}$), respectively. The values of the activation energy for all samples are calculated from the slope of each plot by using the above logarithmic relation. The different values of E_a are listed in Table 1.

Also, the variation of the activation energy with Fe content for the above different regions is shown in Fig. 2(a,b). This figure show simple curves which are identical in both quenching and slow cooling for each particular case. However, these curves are not absolutely symmetric to the response of high temperature range (300–525 K), suggesting that the high values of E_a at low temperature could be observed. The activation energy for pure ZnO samples obtained in this study is close to (0.1–0.4 eV). It is noteworthy that Fe increased the E_a of ZnO pure sample to higher values. The optimum value of Fe content corresponding to higher E_a is found to be 0.30. The values of E_a are decreased around this value. However, in Schottky-type barrier, the resistivity is related to the electron concentration in the bulk and to the barrier height Φ_B as, $\Phi_B \propto (n/\Phi_B)^{1/2}$. A diminution in the resistivity could then be ascribed to an increase in the potential barrier height, to a decrease in the donor concentration or eventually, to both phenomena occurring simultaneously. Therefore, the effective activation energy as well as the potential barrier height is raised when Fe is incorporated to the barrier formation at the grain–grain interface. When the Fe doping is increased, the E_a is significantly raised; observation that would account for the arising of atomic defects electrically active at grain boundary arises that heightens the potential barrier; in agreement with our previous work [14]. On the other hand, it is noted that the values of E_a for slowly cooled samples are higher than that of quenching.

3.3. Low temperature measurements

Fig. 3(a and b) shows the variation of dc electrical conductivity $\ln \sigma$ of pure and Fe doped ZnO samples with temperature as $1000/T$ ($20\text{K} \leq T \leq 300\text{K}$) in both quenching and slow cooling. The lower conductivity which is observed by Fe doping can be understood as the consequence of high porosity and small grain size. The jumps observed in the conductivity curves can be related with the process of adsorption–desorption of oxygen. This jump practically disappears in ZnO pure samples. This can be related with a high porosity responsible for a better oxygen adsorption which increases the intergranular barrier heights origination a lower conductivity. Fig. 3(c) shows the variation of the onset temperature T_{on1} of the first jump as a function of Fe content in both quenching and slow cooling. It is observed that T_{on1} increased by increasing Fe from 0.00 up to 0.30, followed by a decrease at Fe = 0.50. Similar behavior could be observed for the T_{on2} of the second jump, see Fig. 3(d). Also, the values of onset temperatures

are found to be higher in quenched samples than in slowly cooled samples. However, the behaviors of these jumps against Fe content are typically recorded by the authors for the nonlinear coefficients based on the same batch of samples [14]. We associated this modified behavior to the creation of point defects due to solid solution of Fe in to the host lattice. Excluding the jumps, the character of conductivity shown in Fig. 3 is divided into four different regions over the temperature intervals as follows; ($175\text{K} \leq T \leq 300\text{K}$), ($120\text{K} \leq T \leq 175\text{K}$), ($60\text{K} \leq T \leq 120\text{K}$) and ($15\text{K} \leq T \leq 60\text{K}$), respectively.

It is interesting to mention that conductivity is slightly lower for slowly cooled samples than quenched samples. This behavior may be related to the shape of the intergranular Schottky barrier. Indeed, these barriers are expected to be wider in samples slowly cooled than in those that are quenched [24]. It is known that defects are mostly oxygen vacancies and Zn interstitials [25,26]. Since the measured conductivity is higher for quenched samples, the oxygen vacancies may be higher in slowly cooled samples. Then, the Zn interstitials must be the dominant defect controlling the sample conductivity. The low concentration values of electrically active defects in slowly cooled samples gives rise to a wide depletion layer. However, it has been reported that oxygen is mostly adsorbed at low temperatures in ZnO varistor at the end of the cooling process when the Schottky barriers are already formed [27,28]. So, the strong field at grain boundaries in quenched samples helps oxygen in diffusion. Fig. 4(a,b) shows the variation of the activation energy with Fe content for the above regions. Similar values of E_a are listed in Table 2. It is noteworthy that the behavior of E_a at low temperature is identical in both quenching and slow cooling. But the values of the E_a of quenched samples are higher than slowly cooled samples, which

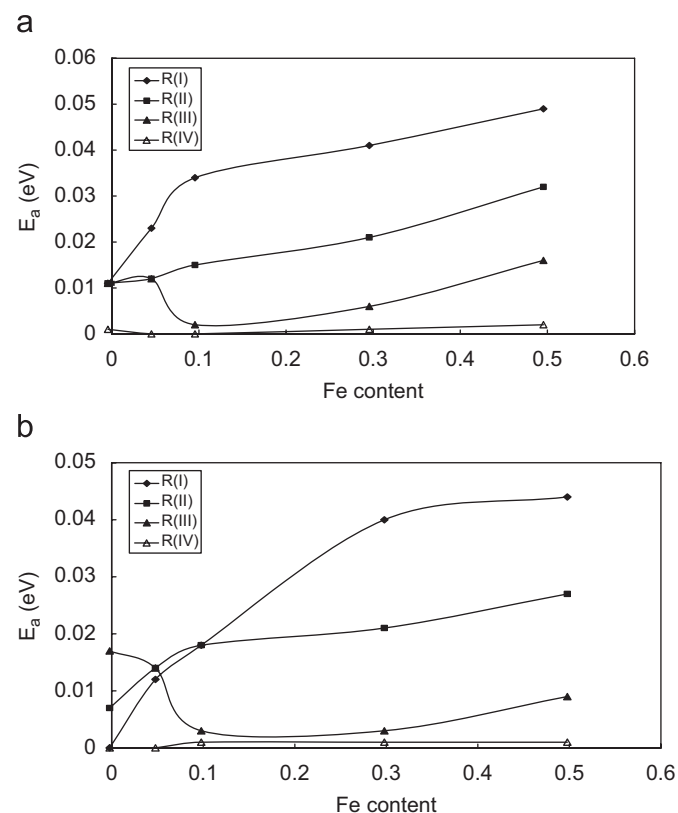


Fig. 4. (a) Activation energy versus Fe content for $\text{Zn}_{1-x}\text{Fe}_x\text{O}$ quenched samples at high temperatures: LT quenching and (b) activation energy versus Fe content for $\text{Zn}_{1-x}\text{Fe}_x\text{O}$ slowly cooled samples at low temperatures: LT slow cooling.

Table 2

E_a versus Fe content at low temperature for $Zn_{1-x}Fe_x$ samples in both quenching and slow cooling.

Fe content	E_a (I) eV (300–175 K)	E_a (II) eV (175–120 K)	E_a (III) eV (120–60 K)	E_a (IV) eV (60–15 K)
Quenching				
0.00	0.011	0.011	0.011	0.001
0.05	0.023	0.012	0.012	0.000
0.10	0.034	0.015	0.002	0.000
0.30	0.041	0.021	0.006	0.001
0.50	0.049	0.032	0.016	0.002
Slow cooling				
0.00	0.012	0.007	0.017	0.000
0.05	0.018	0.014	0.014	0.000
0.10	0.040	0.018	0.003	0.001
0.30	0.049	0.021	0.003	0.001
0.50	0.044	0.027	0.009	0.001

indicate that the grain size response to the temperature variation is more suitable in slow cooling than quenching.

4. Conclusion

The electrical conductivity measurements of $Zn_{1-x}Fe_xO$ ceramic samples are reported in both high and low temperature case. Furthermore, the activation energies are calculated from the conductivity curves for the considered samples. Generally, the conductivities are increased over the temperature range selected in both cases. While, these values are decreased with the increase in the Fe content up to $Fe = 0.50$. In high temperature case, the values of E_a are increased with increasing Fe up to 0.30, followed by a decrease at 0.50. While in low temperature case, the values of E_a are generally increased with increasing Fe up to 0.50. We believe that potential barrier, donor concentration, point defects and adsorption–desorption of oxygen are the main reasons which are controlling the conductivity of ZnO ceramic system.

Acknowledgment

The authors would like to thank the Deanship of Scientific Research, King Faisal University for providing facilities and maintenance support during the present work.

References

- [1] T.K. Gupta, *J. Am. Ceram. Soc.* 37 (7) (1990) 1817.
- [2] D.R. Clarke, *J. Am. Ceram. Soc.* 82 (3) (1999) 485.
- [3] M. Matsouka, *Jpn. J. Appl. Phys.* 10 (6) (1971) 736.
- [4] J.P. Gambino, W.D. Kingery, G.E. Pike, H.R. Philipp, L.M. Levinson, *J. Appl. Phys.* 61 (7) (1987) 2571.
- [5] K. Mukae, K. Tsuda, I. Nagasawa, *Jpn. J. Appl. Phys.* 16 (8) (1977) 1361.
- [6] H. Hoon, C.P. Ling, *Mater. Chem. Phys.* 9347 (2002) 1.
- [7] Y.L. Tsai, C.L. Huang, C.C. Wei, *J. Mater. Sci. Lett.* 4 (1985) 1305.
- [8] R. Einzinger, *Appl. Surf. Sci.* 1 (1979) 329.
- [9] F. Greuter, G. Blatter, *Semicond. Sci. Technol.* 5 (1990) 111.
- [10] M.H. Tuller, K.K. Boak, in: L.M. Levinson (Ed.), *Ceramic Transactions, Grain Boundaries and Interfacial Phenomena in Electronic Ceramics*, vol. 41, American Ceramic Society, Westerville, OH, 1994, p. 19.
- [11] I. Shuratovsky, A. Glot, E. Di Bartolomeo, E. Traversa, R. Polini, *J. Eur. Ceram. Soc.* 24 (9) (2004) 2597.
- [12] J. Han, P.Q. Mantas, A.M.R. Senos, *J. Eur. Ceram. Soc.* 22 (2002) 49.
- [13] Z. Zhou, K. Kato, T. Komaki, M. Yoshino, H. Yukawa, M. Morinaga, K. Morita, *J. Eur. Ceram. Soc.* 24 (2004) 139.
- [14] A. Sedky, M. Abu-Abdeen, A.A. Almulhem, *Phys. B: Condens. Matter*, submitted.
- [15] J. Han, P.Q. Mantas, A.M.R. Senos, *J. Eur. Ceram. Soc.* 21 (2001) 1883.
- [16] W.G. Carlson, T.K. Gupta, *J. Appl. Phys.* 53 (1982) 5746.
- [17] N. Ohashi, Y. Terada, T. Ohgaki, S. Tanaka, T. Tsurumi, O. Fukunage, H. Haneda, J. Tanaka, *Jpn. J. Appl. Phys.* 38 (1999) 5028.
- [18] F. Oba, I. Tanaka, H. Adachi, *Jpn. J. Appl. Phys.* 38 (1999) 3569.
- [19] P.Q. Mantas, J.L. Baptista, *J. Eur. Ceram. Soc.* 15 (1995) 605.
- [20] J. Han, A.M.R. Senos, P.Q. Mantas, *J. Eur. Ceram. Soc.* 22 (2002) 1653.
- [21] J. Han, A.M.R. Senos, P.Q. Mantas, *J. Eur. Ceram. Soc.* 19 (1999) 1003.
- [22] J. Han, A.M.R. Senos, P.Q. Mantas, *Mater. Chem. Phys.* 75 (2002) 117.
- [23] J. Han, P.Q. Mantas, A.M.R. Senos, *J. Eur. Ceram. Soc.* 22 (2002) 49.
- [24] M.S. Castro, C.M. Aldao, *J. Eur. Ceram. Soc.* 19 (1998) 511.
- [25] F. Morazzoni, R. Scotti, S. Volonte, *J. Chem. Soc. Faraday Trans.* 86 (1990) 1587.
- [26] M.H. Sukar, H.L. Tuller, in: M.F. Yan, A.H. Hever (Eds.), *Advances in Ceramics*, vol. 7 (71), 1984.
- [27] K. Tanaka, G. Blyholder, *J. Phys. Chem.* 76 (1972) 3184.
- [28] M. Kobayashi, T. Kanno, T. Kimura, *J. Chem. Soc. Faraday Trans.* 84 (1988) 2099.